RESEARCH ARTICLE

Open Access

A Robust Low Cost Device for Measuring Road Induced Vibrations

Greg Mason[1]✉, Mike Larson[1], Ricky Deng[1], Dalton Reed[1], Marie Pahlmeyer[1], Nicholaus Wright[1], Zu Pong Wu[1] and Jayce Yahata[1]

Abstract

Road induced vibrations may be linked to cycling comfort and fatigue. Currently, vibration tests are preformed using expensive equipment which is often unsuitable for tests involving large numbers of cyclists riding in real-world conditions in inclement weather. A robust low-cost device was developed to address this shortcoming. The device is capable of measuring vibrations at two locations for extended periods of time. Data collected includes acceleration frequency spectrum and GPS coordinates. The system uses a custom hardware based on readily available components, costing approximately 100 USD, and a smartphone. It weighs 135 g, plus the weight of the smartphone, and can collect data for over 12 hours on a single charge. Two types of tests were used to validate the system. A controlled test with a single rider showed that the device can be used to measure differences in the RMS of the acceleration frequency spectrum for a bicycle ridden over chipseal road with a difference in tire pressures of less than 0.7 bar. Extended tests on a commuter bicycle over a six week period were also successfully performed to verify that the device could endure an urban commute in inclement weather.

Keywords: vibration, acceleration, cycling comfort, road surface mapping

✉ **Contact email:** *mason@seattleu.edu* (G. Mason)

[1] *Department of Mechanical Engineering. Seattle University, United States*

Received: 23 September 2015. Accepted. 17 March 2016.

Introduction

Monitoring of bicycle performance has become increasingly important in cycling research. Performance data, specifically, vibration data is believed to be correlated to rider comfort and fatigue (Hastings et al., 2004; Torbic et al., 2003; Ayachi et al., 2015). Understanding the effects of vibrations on ride comfort can help cyclists make informed decisions on how to configure their bicycle to achieve the right balance of comfort and performance. This type of data is useful to avid recreational cyclists as well as competitive cyclists. The instrumentation described in this paper was developed specifically to study the relationship between road surface induced vibrations, rider comfort, tire size, and tire pressure. In addition, data from longitudinal studies can be used to track road conditions and help cyclists and government officials plan and maintain cycling routes.

Several researchers have published designs for monitoring vibrations induced by road surface irregularities. Hölzel et al. (2012) measured rider comfort and rolling resistance on different road surfaces and were able to correlate rider comfort with vibrations measured at the seat. Their system used an onboard mini-pc and hardware from National Instruments. Oliemana et al. (2012) developed a system that transmitted acceleration data using a dedicated high-speed network and wireless transmitters. Giubilato and Petrone (2012) measured wheel vibration using piezoelectric accelerometers and an industrial data acquisition system. Vanwalleghem et al. (2012) developed an instrumented bicycle to evaluate rider comfort. That system utilized strain gauges to measure deflection and vibration, a National Instruments data acquisition card and a laptop computer. All of these systems were designed for a laboratory type setting in controlled environments and so are limited when applied to real-world conditions.

Numerous researchers have participated in the Instrumented Probe Bicycle (IPB) project. The goal of that project is to develop reliable bicycle instrumentation to automate real-world data collection. Although not specifically targeting vibrations, some of these bicycles do include vibration measurement equipment. Mohanty et al. (2014) summarized global IPB research and highlighted research by Vanwalleghem et al. (2013) and Yamanaka et al. (2013) that included vibration measuring instruments in their designs. One notable IPB system was implemented by Bíl et al. (2015). This system was designed for use outside of a laboratory setting. It used a Garmin GPS and a portable battery powered data logger. The data logger included an accelerometer and built-in memory so acceleration readings could be collected and later downloaded to a computer. The system however was limited to collecting acceleration data at frequencies below 10 Hz and required post processing of data to synchronize GPS coordinates and accelerometers' data.

While all of the aforementioned systems were successfully used to collect vibration data, all were either too expensive or impractical to be installed on multiple bicycles and used for long term tests on bicycles in real-world conditions. This paper describes a new low-cost system for measuring road vibrations. The system was designed to be inexpensive and durable. It can be easily installed on multiple bicycles and can be used for extended periods of time with minimal user attention.

Equipment

The road vibration measurement system is designed to measure and record vibrations at two locations and associate those data with GPS information. A schematic of the system is shown in Figure 1.

Figure 1. Schematic of the vibration monitoring system

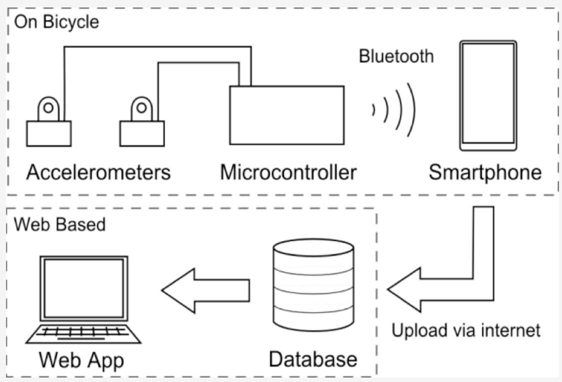

Accelerometers are MEMS based devices (MMA7361L) with a 400 Hz bandwidth, a ±6 g range and a 200 mV/g sensitivity. The device is low cost and can be purchased pre-mounted on a small circuit card. Although the MMA7361L is a three axis accelerometer, only a single axis of the accelerometer is used for this system. The accelerometers are oriented to measure accelerations perpendicular to the road. On a level surface this results in a nominal range of −7 g to +5 g parallel to the acceleration of gravity. While cyclists can experience accelerations well above the range of this accelerometer on rough roads (Olieman et al. 2012), in tests using commuters riding at speeds between 15 km/h and 30 km/h on typical roads in downtown Seattle, WA, less than 5% of measurements exceed the limits of the accelerometer. For road conditions resulting in higher accelerations, the MMA7361L could be substituted for a MMA2202KEG accelerometer. That device has a ±50 g range and a 40 mV/g sensitivity. The cost of the MMA2202KEG is similar that of the MMA7361L, however it is not readily available pre-mounted on a circuit card and the accelerometer has a lower sensitivity than the accelerometer currently in use.

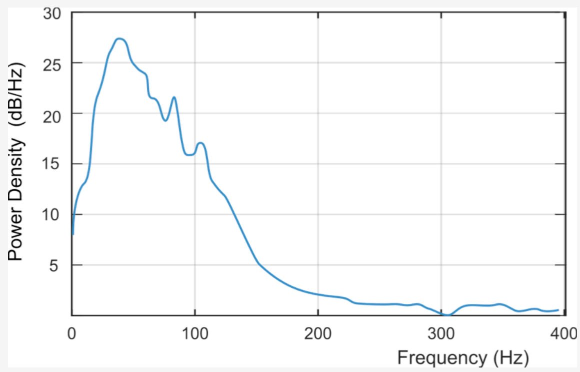

Figure 2. Frequency domain plot of typical test ride where power is in units of m^2/s^4

The system was designed with a capability to monitor two accelerometers in order to provide flexibility in future studies. For example, one accelerometer could be mounted directly on the seat post to measure vibrations transmitted through the frame to the seat and another mounted to a wheel axle to measure the effects of wheel and tire configurations. In this paper all results were reported for a single accelerometer mounted on the front axle.

Acceleration data is sampled at 1.6 kHz and processed using an 80 MHz PIC32 microcontroller. The accelerometer is band limited by an internal low pass filter with a cutoff at 400 Hz. This cutoff is above the frequencies measured on test rides. Those frequencies are typically below 200 Hz. A frequency spectrum of a typical ride is shown in Figure 2.

The 1.6 kHz sample frequency ensures that even the fastest signals from the accelerometer are not aliased. The microcontroller calculates the frequency response of the acceleration data using a 1024 point FFT. The size of the FFT is limited by the available memory on the microcontroller. The resulting spectrum is computed every 0.640 seconds (1.6 kHz × 1024 samples) with a resolution of 1.56 Hz and a range of 0 Hz to 800 Hz. The spectral data point at 0 Hz corresponds to the DC component of the acceleration signal and is not used in this paper.

The microcontroller then transmits spectral data through a Bluetooth connection to a smartphone. Because transmitting all the spectra data every 0.64 seconds exceeds the bandwidth of the Bluetooth connection, the discrete spectral data is reduced to 16 data points, S_p^2, for each accelerometer, where

(1)
$$S_p^2 = \sum_{\omega=\omega_{lower,p}}^{\omega_{upper,p}} A^2(\omega) \text{ for } p = 0,1,2,\ldots,15$$

$\omega_{lower,p}$ and $\omega_{upper,p}$ are upper and lower frequencies used to calculate S_p^2, and $A(\omega)$ is the corresponding intensity value from the discrete Fourier transform. The ranges for each S_p^2 can be of non-uniform size ($\omega_{upper,p} - \omega_{lower,p}$ is not constant for all p), and can be changed for each application. However, $\omega_{lower,p}$ to $\omega_{upper,p}$ ranges cannot overlap for any two values of p, and the sum of all $\omega_{upper,p} - \omega_{lower,p}$ for all p's must equal 800 Hz. That is, the 16 values for S_p^2 must uniquely account for all frequencies in the discrete spectral data. The exception is the data point associated with 0 Hz, which can be ignored if the DC component of the signal is not being used in future analysis. For the analysis presented later in this paper, S_p^2 were chosen to be approximately equally spaced along a logarithmic frequency scale. Those values are shown in Table 1. Data collection, FFT calculations and Bluetooth communication occur asynchronously on the microcontroller to minimize the effects of computational and communication delays on data sampling.

The smartphone uses a custom Android app to determine the latitude and longitude of the cyclist and pair that with the corresponding spectral data. GPS coordinate information is provided by the location services built into the Android operating system and is updated every 0.640 seconds. The location services on the Android operating system uses information from GPS, cell towers and WiFi hot spots to determine the phone's GPS coordinates (Android Developer API 2015). Data containing the current time, acceleration spectral data, GPS coordinates and rider speed, calculated from GPS coordinates, are stored on the phone in a comma separated (CSV) data file. Storage for two accelerometers and GPS data requires approximately 1.2 MB/h.

The data stored on the smartphone can be uploaded to a remote server using a custom web app or it can be opened directly using software such as Microsoft Excel or MATLAB®. Users can collect multiple data sets before uploading data to the server since the data is stored on the phone's internal storage. Storing data locally on the smartphone means that the phone does not need a persistent connection to the internet. This was a key design consideration since the system is designed to collect data in areas without cell phone service.

Table 1 Frequency ranges for S_p used in this study

p	Frequency Range (Hz)	p	Frequency Range (Hz)
0	0 ≤ F < 1.56	8	20.3 ≤ F < 29.7
1	1.56 ≤ F < 3.12	9	29.7 ≤ F < 42.2
2	3.12 ≤ F < 4.68	10	42.2 ≤ F < 60.9
3	4.68 ≤ F < 6.24	11	60.9 ≤ F < 89.1
4	6.25 ≤ F < 7.81	12	89.1 ≤ F < 129
5	7.81 ≤ F < 9.37	13	129 ≤ F < 189
6	9.37 ≤ F < 14.1	14	189 ≤ F < 275
7	14.1 ≤ F < 20.3	15	275 ≤ F < 800

Once the data has been uploaded to the server, users can access the data using any browser and a custom web app. The web app can recall raw test data or plot the data on a map. An annotated screen capture from the web app is shown in Figure 3. The upper map shows the cyclists route. The lower graph shows the RMS of acceleration, R_t, and speed vs time, where

(2)

$$R_t = \sqrt{\frac{1}{N}\sum_{i=0}^{N-1} af_i^2}$$

af_i is the frequency weighted sampled value of acceleration at the i^{th} sampling time, and N is the number of samples (1024 for this system). This value is calculated directly from the frequency spectra using Parseval's Theorem. Because accelerations are stored as S_p^2 values for a distinct range of frequencies, it is straightforward to apply an appropriate frequency weighting, such as those prescribed in the ISO standard 2631 (ISO 1997) or 5349 (ISO 2001), appropriate to the application and accelerometer placement.

Figure 4 shows the system components (except for the smartphone). For tests described in this paper, the accelerometers are mounted to aluminum tabs, encased in epoxy potting compound and sealed in plastic cases. They are then mounted to the bicycle at the axles. The mounting tab has a nominal 5 mm hole that provides clearance for the skewer shaft on a quick-release mechanism. The accelerometer is mounted as shown in Figure 4 (right) with the base of the case parallel to level ground. This ensures that acceleration measurements are perpendicular to the bicycle. Nominal measurements can be taken using the microcontroller and smartphone immediately after mounting to verify the orientation of the accelerometer. The microcontroller and battery measures

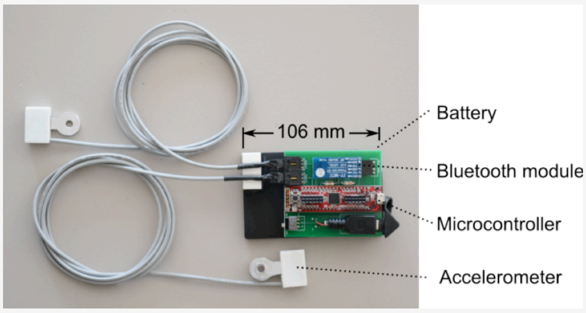

Figure 4. (Left) Data acquisition hardware. (Right) Accelerometer mounted on rear axle

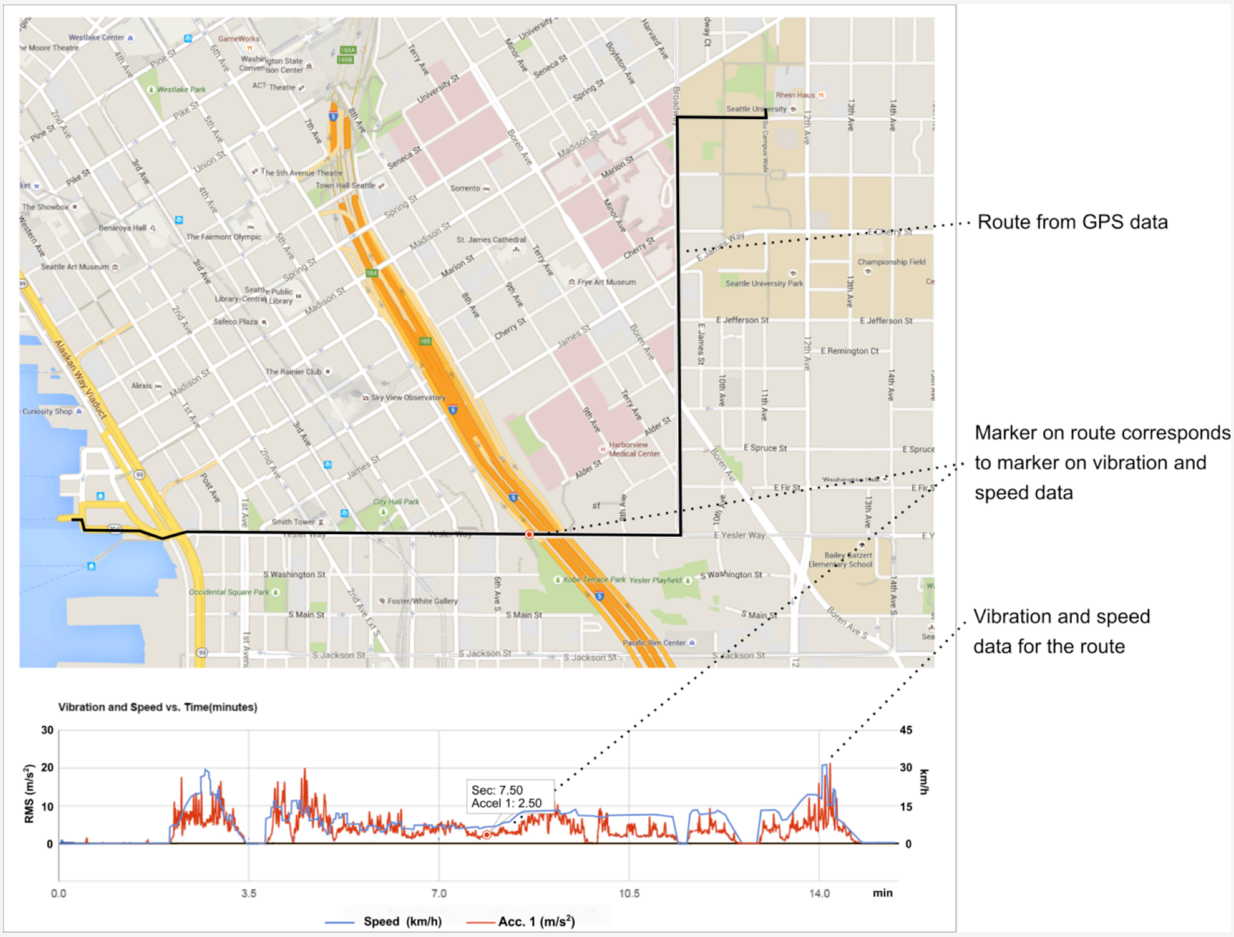

Figure 3. Web App screen capture showing a segment of bicycle commuter's route from ferry terminal to downtown Seattle. Commuter was using a single accelerometer on the front axle.

103 mm x 64 mm x 25 mm and can be stored in a small bag under the seat. The system, excluding smartphone, weighs 135 g and can run for over 12 hours on a single charge. In general, the smartphone battery life is the limiting factor on rides of long duration. Total cost of hardware is approximately 100 USD. This does not include the cost of the ubiquitous smartphone.

Results

The system was tested on a straight, 150 m segment of pavement using an aluminum road bicycle with 25 mm wide tires pressurized to 6.21 bar (90 psi). The total mass of rider and bicycle was 86 kg. The pavement was chipseal road with nonhomogeneous surface roughness. In places, the surface had exposed aggregate. A typical rider would likely consider this surface rideable, but would avoid it if there were an alternate route. For this test, only values from an accelerometer mounted on the front axle are presented. To perform the test, the rider began from a stop, accelerated down a mild grade to 26 km/h and then decelerated up a mild grade at the end of the ride.

Figure 5 shows the frequency content with respect to time for a typical trial. The time axis corresponds to the time along the route. R_{freq} is the RMS value of acceleration at the indicated frequency. No frequency weighting was applied to the tests in this paper since the goal of the tests was only to demonstrate the capabilities of the system. Note that the frequency axis is based on a log scale. The increase in R_{freq} near 30 seconds coincides with the roughest section of the road, and the time at which the riders speed was the highest.

As expected, dominate vibrational frequencies occurred below 200 Hz. This coincides with results shown in Figure 2 , is well below the 400 Hz roll-off of the sensor, and is 8 times slower than the 1.6 kHz sampling rate.

To demonstrate the systems sensitivity and repeatability, the same route was ridden six times for three different tire pressures. Six trials were ridden at 6.21 bar (90 psi), six at 6.89 bar (100 psi), and six at 7.58 bar (110 psi). The test was performed by an experienced rider. Speeds were very consistent with less than a 2% variation in time between runs. R_{total} was computed for each test where

(3)

$$R_{total} = \sqrt{\frac{1}{M}\sum_{i=0}^{M-1} R_t^2(i)}$$

$R_t(i)$ is R_t for a given 0.640 seconds time interval and M is the number of R_t values collected during a given test. The results are presented in Table 2.

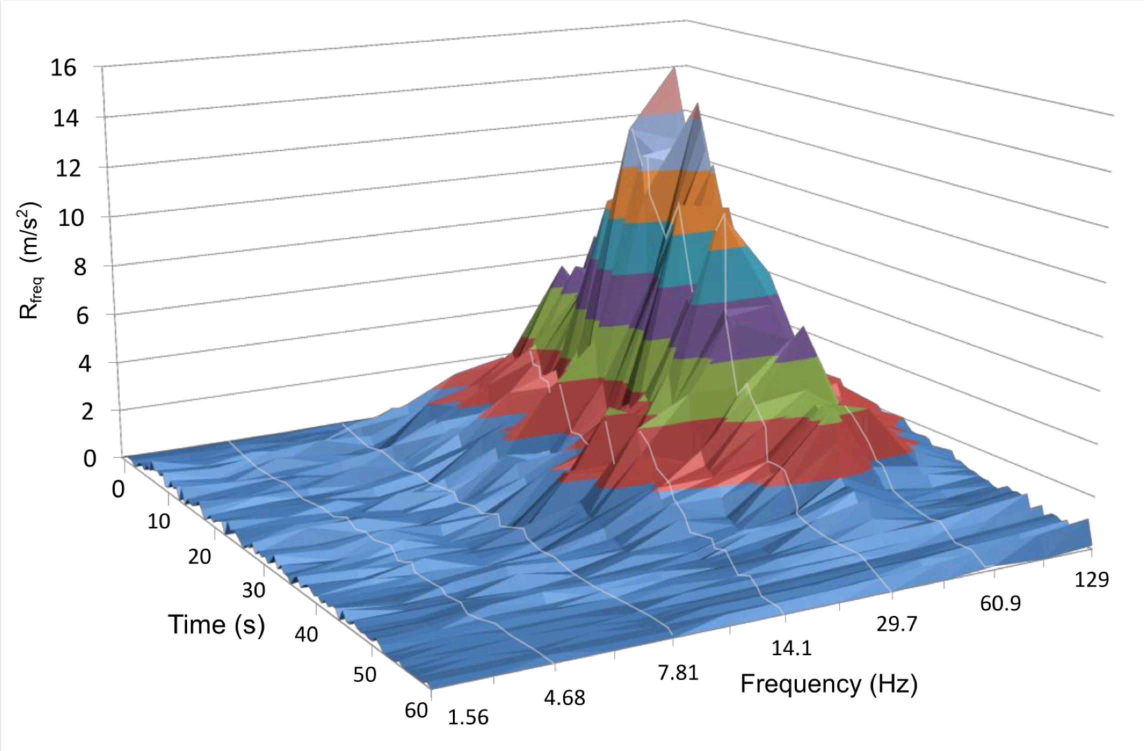

Figure 5. RMS verses time for a typical test ride. Accelerometer was mounted on front axle. Frequencies above 129 Hz have an R_{freq} less than 1 m/s^2 and are not shown.

Figure 6 shows the total R_t over the same route shown in Figure 5. Recall that R_t represents the RMS of the accelerations over a 0.64 second interval.

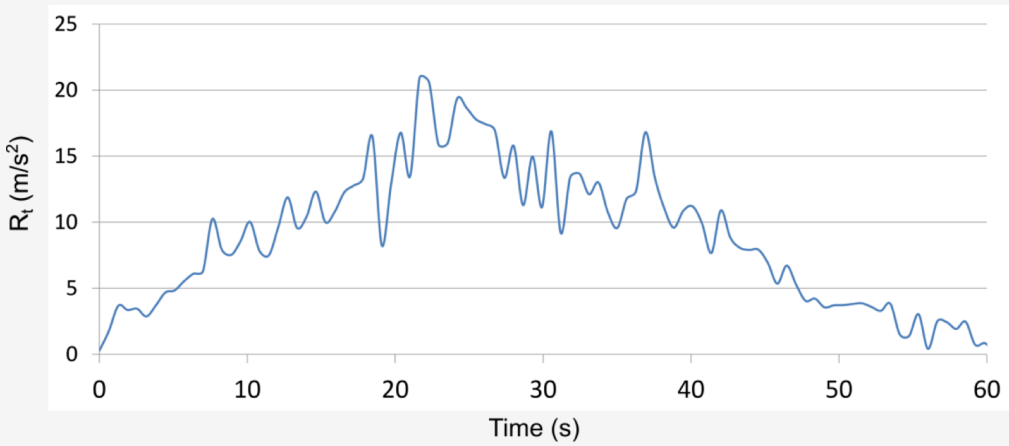

Figure 6. R_t and speed for typical test ride. See Figure 5 for spectral data for this test

Table 2. Results from test runs using three different tire pressures

Tire Pressure	n	Average Rtotal (m/s^2)	Variance (m^2/s^4)
6.21 bar (90 psi)	6	10.03	0.068
6.89 bar (100 psi)	6	10.41	0.102
7.58 bar (110 psi)	6	11.49	0.300

A single factor ANOVA analysis supplemented with a Tukey-Kramer test showed a significant difference (p-value <0.05) between all groups except the 6.21 bar (90 psi) to 6.89 bar (100 psi) comparison. The ANOVA results, however, may be biased due to the unequal variances of the groups. A direct comparison of adjacent groups showed a significant difference in means between both the 6.21 bar (90 psi), 6.89 bar (100 psi) groups (p-value=0.048) and the 6.89 bar (100 psi), 7.58 bar (110 psi) groups (p-value=0.002). The results suggest that the system is sensitive enough to identify differences in R¬¬total due to pressure differences of 0.69 bar (10 psi).

Finally, to test the durability of the device, it was installed on two commuter bicycles and used to collect data over a six week period. Commuters road an average of 20 km round trip in Seattle (USA) traffic, each day, in both wet and dry weather. Commuters did not report any significant problems with the system and were able to successfully record and upload data to the server. A partial commute route was previously shown in Figure 3.

Conclusions

The vibration monitoring device described in this paper provides a robust, low cost method for collecting vibration data in real-world conditions. The device is inexpensive enough that it can be distributed to multiple cyclists for data collection over extended periods of time. Since test data is stored in a database as spectral data, it is straightforward to apply different frequency weights to the results after the data has been collected. Appropriate weighting values for a given application are prescribed in the ISO standards 2631 (ISO 1997) and 5349 (ISO 2001). The current system is limited by the ±6 g accelerometer. While that accelerometer is adequate for current test conditions, a higher g accelerometer should be used when testing on rougher road surfaces, at higher speeds or when monitoring extremes in road conditions. In the future, the authors plan to add a high resolution speedometer to supplement GPS speed data. Higher resolution speed data will be used to account for differences in vibration intensity due to rider speed when tests are not being performed in controlled conditions, as was the case in this paper. The device will then be used to measure and record road conditions in the Seattle area. Data for a given route will be collected using different tire sizes and air pressures and then correlated with reported rider comfort. Additional modifications may be made to the web app interface to ensure privacy if the system is implemented in a public study.

Acknowledgements

This work was funded in part through the PACCAR Endowed Chair, Department of Mechanical Engineering, Seattle University, and through the Seattle University Design Center.

References

1. Android Developer API (2015), Location Services, http://developer.android.com/guide/topics/location/index.html
2. Ayachi F.,Dorey J, Guastavino C (2015) Identifying factors of bicycle comfort: an online survey with enthusiast cyclists, Appl. Ergon., 4, pp. 124–136
3. Bíl M, Andrášik R, Kubeček J (2015), How comfortable are your cycling tracks? A new method for objective bicycle vibration measurement, Transportation Research Part C: Emerging Technologies, Volume 56, Pages 415–425
4. Hastings A, Blair B, Culligan K, Pober M (2004) Vibration Measuring the effect of transmitted road vibration on cycling performance, Center fir Sports Innovation, Massachusetts Institute of Technology, Cambridge, MA, USA, Department of Exercise Science, University of Massachusetts, Amherst, MA, USA <http://web.mit.edu/2.tha/www/ppt/Bike-ISEA.pdf>
5. Hölzel C, Höchtl F, Senner V (2012), Cycling comfort on different road surfaces, Procedia Eng., 34, pp. 479–484
6. Giubilato F, Petrone N (2012), A method for evaluating the vibrational response of racing bicycles wheels under road roughness excitation Procedia Eng., 34 (2012), pp. 409–414
7. ISO, International Organization for Standardization, (1997), Mechanical vibration and shock—Evaluation of human exposure to whole body vibration—part 1: general requirements, ISO 2631-1:1997.
8. ISO, International Organization for Standardization, (2001), Mechanical vibration — Measurement and evaluation of human exposure to hand-transmitted vibration —Part 1: general requirements, ISO 5349-1:2001
9. Mohanty, S., Lee, A., Carvalho, T., Dias, L., Lovegrove, G. (2014) A global review of current Instrumented Probe Bicycle (IPB) technology and research. In: International Cycling Safety Conference 2014 18–19, Gothenburg, Sweden. 15 pp.
10. Olieman M, Marin-Perianu R, Marin-Perianu M (2012), Measurement of dynamic comfort in cycling using wireless acceleration sensors Procedia Eng., 34, pp. 568–573
11. Torbic D, El-Gindy M, Elefteriadou L (2003), Methodology for quantifying whole-body vibration experienced by bicyclists, International Journal of Vehicle Design, 4, pp. 452–480
12. Vanwallenghem J, Mortier F, De Baere I, Loccufier M, Van Paepegem W (2012), Design of an instrumented bicycle for the evaluation of bicycle dynamics and its relation with the cyclist's comfort, Procedia Eng., 34, pp. 485–490
13. Vanwalleghem, J,. De Baere, I, Loccufier, M. Van Paegegem (2013) Sensor design for outdoor racing bicycle field testing for human vibration comfort evaluation, Measurement Science and Technology, 24(9)
14. Yamanaka, H., Pan, Z., Sanada, J (2013) Evaluation models for cyclists' perception using probe bicycle system , Proceedings of the Eastern Asia Society for Transp. Studies, 9.